Atmos. Meas. Tech. Discuss., 6, 2227–2251, 2013
www.atmos-meas-tech-discuss.net/6/2227/2013/
doi:10.5194/amtd-6-2227-2013

Atmospheric Measurement Techniques
Open Access
Discussions

Retrieval of aerosol optical depth over land surfaces from AVHRR data

L. Mei[1,2,7], Y. Xue[1,3], A. A. Kokhanovsky[2], W. von Hoyningen-Huene[2], G. de Leeuw[4,5,6], and J. P. Burrows[2]

[1]State Key Laboratory of Remote Sensing Science, Jointly Sponsored by the Institute of Remote Sensing Applications of Chinese Academy of Sciences and Beijing Normal University, Institute of Remote Sensing and Digital Earth, Chinese Academy of Sciences, Beijing 100101, China
[2]Institute of Environmental Physics, University of Bremen, Otto-Hahn-Allee 1, 28359 Bremen, Germany
[3]Faculty of Life Sciences and Computing, London Metropolitan University, 166–220 Holloway Road, London N7 8DB, UK
[4]Department of Physics, University of Helsinki, Helsinki, Finland
[5]Finnish Meteorological Institute, Climate Change Unit, Helsinki, Finland
[6]Netherlands Organization for Applied Scientific Research TNO, Utrecht, The Netherlands
[7]University of the Chinese Academy of Sciences, Beijing 100039, China

Received: 29 November 2012 – Accepted: 29 January 2013 – Published: 28 February 2013

Correspondence to: Y. Xue (yxue@irsa.ac.cn)

Published by Copernicus Publications on behalf of the European Geosciences Union.

Abstract

The Advanced Very High Resolution Radiometer (AVHRR) radiance data provide a global, long-term, consistent time series having high spectral and spatial resolution and thus being valuable for the retrieval of surface spectral reflectance, albedo and surface temperature. Long term time series of such data products are necessary for studies addressing climate change, sea ice distribution and movement, and ice sheet coastal configuration. These data have also been used to retrieve aerosol properties over ocean and land surfaces. However, the retrieval of aerosol over land and land surface albedo are challenging because of the information content of the measurement is limited and the inversion of these data products being ill defined. Solving the radiative transfer equations requires additional information and knowledge to reduce the number of unknowns. In this contribution we utilise an empirical linear relationship between the surface reflectances in the AVHRR channels at wavelengths of 3.75 µm and 2.1 µm, which has been identified in Moderate Resolution Imaging Spectroradiometer (MODIS) data. Next, following the MODIS dark target approach, the surface reflectance at 0.64 µm was obtained. The comparison of the estimated surface reflectance at 0.64 µm with MODIS reflectance products (MOD09) shows a strong correlation ($R = 0.7835$). Once this was established, the MODIS "dark-target" aerosol retrieval method was adapted to Advanced Very High Resolution Radiometer (AVHRR) data. A simplified Look-Up Table (LUT) method, adopted from Bremen AErosol Retrieval (BAER) algorithm, was used in the retrieval. The Aerosol Optical Depth (AOD) values retrieved from AVHRR with this method compare favourably with ground-based measurements, with a correlation coefficient $R = 0.861$ and Root Mean Square Error (RMSE) = 0.17. This method can be easily applied to other satellite instruments which do not have a 2.1 µm channel, such as those currently planned to geostationary satellites.

AMTD
6, 2227–2251, 2013

Retrieval of aerosol optical depth over land surfaces from AVHRR data

L. Mei et al.

1 Introduction

Algorithms developed to retrieve aerosol properties from satellite-based instruments use optimally the information available in the passive remote sensing observations of back scattered reflected upwelling radiation , such as the reflectance available at different wavebands, multiple viewing angles and/or polarization. The results further depend on the swath width and spatial and temporal resolution. An overview of aerosol retrieval algorithms and products is provided in Kokhanovsky and de Leeuw (2009), de Leeuw et al. (2011) and Mei et al. (2012). For instance, the most popular "dark-target" approach for MODIS uses the 2.1 µm band to estimate the reflectance for visible bands (Kaufman et al., 1997). The Bremen AErosol Retrieval (BAER) algorithm for MERIS (von Hoyningen-Huene et al., 2003, 2011) utilizes the Normalized Difference Vegetation Index (NDVI). Some dual-view algorithms such as the AATSR-Dual-View (ADV) algorithm (Kolmonen et al., 2013; Curier et al., 2009; Grey et al., 2006), the multi-observation approach for MODIS (Tang et al., 2005; Mei et al., 2013a), Advanced Along-Track Scanning Radiometer (AATSR) (Xue et al., 2009; Mei et al., 2013b) and the Jet Propulsion Laboratory (JPL) algorithm for the Multiangle Imaging Spectroradiometer (MISR) (Diner et al., 2005) are based on the assumption that the surface reflectance can be approximated by a parameter which describes the variation with the wavelength and another one which describes the variation with the geometry (Flowerdew and Haigh, 1995). For geostationary satellites a time series method are employed assuming that the surface reflectance can be selected for each pixel as the second darkest image, in order to avoid cloud shadow, for selected time periods for each pixel (Knapp et al., 2002, 2005) and that the surface reflectance is stable in a short time period (Mei et al., 2012).

One of the most popular methods is the use of an empirical relationship between radiances observed at different wavelengths to obtain the reflectance at wavelengths in the visible band of the electromagetic spectrum. This was first described and applied in the MODIS "dark-target" approach (Kaufman et al., 1997). Similarly, Holzer-Popp et al. (2009) developed a regression function between top-of-atmosphere reflectance at 1.6 µm and the surface reflectance at 0.67 µm and von Hoyningen-Huene et al. (2009) use the empirical relationship between 0.67 µm and 2.1 µm bands for sun glint correction for the Multi Spectral Imager (MSI) instrument (von Hoyningen-Huene et al., 2009). The operational algorithm used to retrieve the AOD over ocean using Advanced Very High Resolution Radiometer (AVHRR) data (Brindley et al., 2005) and the Oxford-RAL Aerosol and Cloud (ORAC) method (Bulgin et al., 2011) were used for MSG/SEVIRI AOD retrieval.

It is challenging to retrieve the aerosol properties from AVHRR data because of the band-setting limitation. However, the use of AVHRR data to retrieve aerosol properties is attractive because the AVHRR satellites have been in continuous polar orbit since 1979 (Holben et al., 1992) and thus provides a unique data series for long-term analysis. Xue and Cracknel (1995) developed one retrieval approach using multi-observation AVHRR data by solving a set of analytical equations. Takemata et al. (2006) derived the surface reflectance at 3.75 µm using the Rojer and Vermote (1998) scheme and then established an empirical relationship between the 0.64 µm and 3.75 µm bands using ground-based measurements. However, only 30 points were used for regression, which limited the algorithm to selected land-cover types or certain areas. However, the surface emissivity is variable, due to changing surface temperatures, which may cause an uncertainty in the relationship between the reflectance at 3.75 and 0.64 µm. Hauser et al. (2005) estimated the surface reflectance from a time series including a period of 44 days and then retrieved AOD using a radiative transfer code. Riffler et al. (2010) improved the method from Hauser et al. (2005) by considering a new surface estimating method as well as the aerosol type. Holben et al. (1992) tried to implement a retrieval algorithm previously developed for Landsat data to that of AVHRR.

In this manuscript, we present a method to retrieve the AOD over land using data from AVHRR data onboard the National Oceanic and Atmospheric Administration (NOAA) satellite. The approach assumes that surface reflectance of 0.64 µm can be obtained using an empirical relationship between the reflectances at that wavelength

AMTD
6, 2227–2251, 2013

and at 3.75 µm, using the MODIS dark surface approach. After correction for surface effects on the Top of Atmosphere (TOA) reflectance, the AOD was derived using a Look-Up Table (LUT) method adopted from BAER algorithm (von Hoyningen-Huene et al., 2003, 2011).

2 The retrieval algorithm

The reflectance at the top of the atmosphere (TOA) can be described as follows (Chandrasekhar, 1950; Kaufman et al., 1997)

$$R_{\mathrm{TOA}}(\lambda,\mu_0,\mu,\varphi) = R_{\mathrm{atm}}(\lambda,\mu_0,\mu,\varphi) + \frac{A_{\mathrm{sfc}}(\lambda)\cdot T_1(\lambda,\mu_0)T_2(\lambda,\mu)}{1-A_{\mathrm{sfc}}(\lambda)\cdot s(\lambda)} \quad (1)$$

where $\theta = \arccos\mu$ is the satellite zenith angle, $\theta_0 = \arccos\mu_0$ is the solar zenith angle, φ is the relative azimuth angle, $R_{\mathrm{TOA}}(\lambda,\mu_0,\mu,\varphi)$ is the contribution of the Earth surface to the TOA reflectance, $R_{\mathrm{atm}}(\lambda,\mu_0,\mu,\varphi)$ is the contribution of the atmosphere reflectance to the TOA reflectance, which contains two parts, the aerosol reflectance $R_{\mathrm{aero}}(\lambda,\mu_0,\mu,\varphi)$ and the Rayleigh reflectance $R_{\mathrm{Ray}}(\lambda,\mu_0,\mu,\varphi)$ (von Hoyningen-Huene et al., 2003). $A_{\mathrm{sfc}}(\lambda)$ is the surface spectral albedo, $T_1(\lambda,\mu_0)$ is transmission of light propagating downward, $T_2(\lambda,\mu)$ is the transmission of light propagating upward from the surface to TOA and $s(\lambda)$ is the atmospheric hemispherical albedo. We can rewrite Eq. (1) as follows:

$$R_{\mathrm{atm}}(\lambda,\mu_0,\mu,\varphi) = R_{\mathrm{TOA}}(\lambda,\mu_0,\mu,\varphi) - \frac{A_{\mathrm{sfc}}(\lambda)\cdot T_1(\lambda,\mu_0)T_2(\lambda,\mu)}{1-A_{\mathrm{sfc}}(\lambda)\cdot s(\lambda)} \quad (2)$$

The aerosol reflectance was estimated using the BAER (von Hoyningen-Huene et al., 2003) approach, Eq. (3). The Raman-Pinty-Verstraete (RPV) Bidirectional Reflectance Distribution Function (BRDF) model (Maignan et al., 2004) was used to estimate $A_{\mathrm{sfc}}(\lambda)$. After removal of the Rayleigh reflectance, the relation between AOD and aerosol reflectance ($R_{aero}(\lambda,\mu_0,\mu,\varphi)$) was used for AOD retrieval (von Hoyningen-Huene et al., 2011).

$$R_{aero}(\lambda,\mu_0,\mu,\varphi) = R_{TOA}(\lambda,\mu_0,\mu,\varphi) - R_{Ray}(\lambda,\mu_0,\mu,\varphi) - \frac{A_{sfc}(\lambda)\cdot T_1(\lambda,\mu_0)T_2(\lambda,\mu)}{1 - A_{sfc}(\lambda)\cdot s(\lambda)} \quad (3)$$

$T_1(\lambda,\mu_0)$, $T_2(\lambda,\mu_0)$ and $s(\lambda)$ can be obtained using the approximate equation from Kokhanovsky et al. (2005). We also used the aerosol phase functions and single scattering albedo from LACE-98 experiment applied in radiative transfer calculations for LUT as described by von Hoyningen-Huene et al. (2011).

The Rayleigh path reflectance (R_{Ray}) is determined by the Rayleigh optical depth, τ_{Ray}, (Frohlich and Shaw, 1980) and the Rayleigh phase function, $P_{Ray}(\Phi)$, as follows:

$$R_{Ray} = \frac{\tau_{Ray} \times P_{Ray}(\Phi)}{4\mu\mu_0} \quad (4)$$

$$\tau_{Ray} = 0.00864\lambda^{-(3.96+0.074\lambda+\frac{0.05}{\lambda})}, \text{ where } \lambda \text{ is the wavelength.} \quad (5)$$

$$P_{Ray}(\Phi) = \frac{3}{4}(1+\cos^2\Phi), \text{ where } \Phi \text{ is the scattering angle.} \quad (6)$$

To obtain the surface reflectance in the AVHRR visible channels (0.64 µm) we follow the method used in the MODIS dark surface approach. However, because AVHRR does not have a 2.1 µm band, we explore the use of the 3.75 µm channels instead. To do this, the relationship between reflectances at 2.1 µm and 3.75 µm using MODIS data needs to be established. Because we assume that TOA reflectance is equal to surface reflectance at both 2.1 µm and 3.75 µm, and do not determine the relationship between surface reflectances at 0.64 µm and 3.75 µm directly in order to avoid using additional reflectance product. We then use the relationship between 2.1 µm and 3.75 µm and the relationship between 2.1 µm and 0.64 µm.

The reflectance of 3.75 µm is given by Eq. (7) (Allen et al., 1990):

$$L(3.75\,\mu m) = \varepsilon(3.75\,\mu m) \times B(3.75\,\mu m) + R_0(3.75\,\mu m)L_0\mu_0 \quad (7)$$

Discussion Paper | Discussion Paper | Discussion Paper | Discussion Paper |

AMTD

6, 2227–2251, 2013

Retrieval of aerosol optical depth over land surfaces from AVHRR data

L. Mei et al.

Title Page
Abstract Introduction
Conclusions References
Tables Figures
◂◂ ▸▸
◂ ▸
Back Close
Full Screen / Esc
Printer-friendly Version
Interactive Discussion

where $L(3.75\,\mu m)$ is the radiance measured at 3.75 µm, $\varepsilon(3.75\,\mu m)$ is the surface emissivity at 3.75 µm, $B(3.75\,\mu m)$ is the Planck function at 3.75 µm, $R_0(3.75\,\mu m)$ is the reflectance at the TOA at 3.75 µm, L_0 is the solar constant and μ_0 is cosine of solar zenith angle.

The relationship between the surface reflectances at 2.12 and 3.75 µm, $R_{Surf}(2.12\,\mu m)$, and $R'_{Surf}(3.75\,\mu m)$ has the form

$$R'_{Surf}(3.75\,\mu m) = a \times R_{Surf}(2.12\,\mu m) + b, \quad (8)$$

where a and b are functions of the Normalized Difference Vegetation Index (NDVI), which is similar as that proposed by Holzer-Popp et al. (2009).

$$a = -0.85 \times (\mathrm{NDVI}) + 0.85 \text{ and } b = 0.05 \times \mathrm{NDVI} - 0.05 \quad (9)$$

The NDVI is determined for AVHRR as $\mathrm{NDVI} = \dfrac{R_0(0.64\,\mu m) - R_0(0.87\,\mu m)}{R_0(0.64\,\mu m) + R_0(0.87\,\mu m)}$. (10)

and $R_0(0.64\,\mu m)$ is the reflectance at the TOA at 0.64 µm and $R_0(0.87\,\mu m)$ is the reflectance at the TOA at 0.87 µm.

The NDVI values as measured by the satellite need to be corrected ($\mathrm{NDVI}_{corrected}$) for AOD effects, where we use the correction proposed by Holzer-Popp et al. (2009):

$$\mathrm{NDVI}_{corrected} = \mathrm{NDVI} + 0.25\tau_0/\mu_0 \quad (11)$$

where τ_0 is the preliminary AOD used for NDVI correction.

Figure 1 demonstrates the good linear relationship between $R'_{Surf}(3.75\,\mu m)$ and $R_{Surf}(2.12\,\mu m)$. Based on the statistical relationship between $R'_{Surf}(3.75\,\mu m)$ and $R_{Surf}(2.12\,\mu m)$ and the empirical relationship between $R_{Surf}(0.64\,\mu m)$ and $R_{Surf}(2.12\,\mu m)$ used in the MODIS Dark-Target algorithm $R_{Surf}(0.64\,\mu m) = 0.5 \times R_{Surf}(2.12\,\mu m)$, we obtain:

$$R_{Surf}(0.64\,\mu m) = 2.5 \times a \times R_{Surf}(3.75\,\mu m) + 2.5 \times b + 0.05 \quad (12)$$

AMTD
6, 2227–2251, 2013

After obtaining the aerosol reflectance according to Eq. (3), AOD was achieved using a simplified LUT method, adopted from BAER algorithm (von Hoyningen-Huene et al., 2003, 2011).

3 Results and validation

3.1 Study area and dataset

Beijing is the capital of China located near the northwest border of the Great North China Plain (see Fig. 2), the region is suffering serious environmental problems caused by fast economical development and the resultant release of pollutants from anthropogenic activity including land use change. In addition to dust transported from Mongolia, which is dominant during the spring and summer, anthropogenic emissions are the main contributor to pollution over Beijing. The pollution levels may become very high due to the location of Beijing at the northern edge of the North China Plain, which is bounded in the north and west by mountain ranges. Winds blowing south or east push pollutants out of the city, while north or west-blowing winds result in pollutants to be concentrated over the city along the mountain front (http://earthobservatory.nasa.gov/IOTD/view.php?id=38290). Many previous researches show that the AOD over Beijing is often around 0.4–0.5 and sometimes even larger than 2.0 (Sundström et al., 2012). The annual average concentration of $PM_{2.5}$ is about 101 $\mu g\,m^{-3}$ in 2001 (He et al., 2001) while it is about 149 $\mu g\,m^{-3}$ in 2004 (Guinot et al., 2007).

As a result of the relatively large AVHRR swath of approximately 2400 km, the NOAA platforms view the same Earth location twice a day (ascending and descending). In this work, only two channels (0.64 µm and 3.75 µm) of the AVHRR instrument (Ascending) on board the polar orbiting NOAA-18 (June and July 2006–2010) and NOAA-19 (June and July 2011) satellite are used. MODIS level 2 aerosol products (MOD04) and surface reflectance products (MOD09) were used for the comparison of retrieved AOD and surface reflectance derived from AVHRR. For evaluation of the retrieved AODs,

AMTD
6, 2227–2251, 2013

sunphotometer data from the AERONET (Holben et al., 1998) sites at Beijing, Xianghe and Xinlong are used.

3.2 Result and validation

A comparison between the TOA reflectances obtained from AVHRR measurements at 0.64 µm and those for MODIS at 0.66 µm (MOD09), as well as the respective surface reflectances, is shown in Fig. 4 for 9 June 2008. Figure 4 shows that the estimated AVHRR reflectance is quite similar to the MOD09 reflectance product (8 days composite). Note that the MOD09 product was resized to the same spatial resolution as AVHRR. Figure 5 shows the strong correlation between AVHRR and MODIS reflectances.

The AOD at 0.64 µm retrieved from AVHRR data over China, using the method presented above, are shown in Fig. 6 for clear days on 8 and 9 June 2008. The AOD has values of 0.5 and higher, in good agreement with in situ measurements. The highest AOD values occur in the Haidian District, Beijing, which can be explained by the high population density in this area with universities and technology parks. Figure 6 also shows the high AOD to the southwest of Beijing, which contributes to the pollution in Beijing due to transport; see the wind directions indicated in Fig. 7, showing that the governing wind direction was from the southwest. Figure 7 also shows the relative humidity (right) on 9 June 2008 (http://envf.ust.hk/dataview/gts/current/query_gts_series.py?src_type=ax). For instance, the humidity in the south part is about 60 % while it is about 40 % in the north part. A lot of farmland is located to the southwest part of Beijing where during summer, the harvest time for crops such as wheat, biomass burning causes high AODs.

In some areas the AVHRR-derived AOD is underestimated, such as in the area in Fig. 6 indicated by the red circle area and confirmed by AERONET comparison. Ignatov (2002) investigated the calibration uncertainty of NOAA-14 AVHRR and estimated the uncertainty in calibration slope is ±5–10 %. The calibration is better for NOAA-18 (launched in 2005) and NOAA-19 (launched in 2009) used in the paper, however,

AMTD
6, 2227–2251, 2013

calibration problem still exists. If an uncertainty of the calibration causes an increase of the TOA reflectance then this will lead also to an increase of the surface reflectance (Hauser et al., 2005), thus causing a decrease of AOD estimation. Besides the calibration problem, there are two possibilities which may cause this underestimation. One could be overestimation of the surface reflectance and the other could be the use of inappropriate aerosol optical properties in the LUTs. Figure 4 shows that the estimated surface reflectance agrees quite well with MOD09 product in the red circle area. Hence it is likely that the underestimation is caused by the use of inappropriate aerosol optical properties in the LUT. The absorption is not treated very well in the BAER LUT. Comparison with AERONET data shows that for all match-ups in the Beijing area, the AODs from AVHRR were underestimated. This is similar to earlier findings using the BAER LUT (von Hoyningen-Huene et al., 2011). The very high AOD value observed in the study area on 8 June 2008 is due to insufficient cloud screening.

The AOD values at 0.64 µm retrieved with our algorithm were evaluated by comparison with collocated sun photometer data provided by the AERONET sites in Beijing, Xianghe and Xinlong. Results are shown in Fig. 8. The overpass time for each site was queried on the AVHRR homepage. We follow the validation method presented by Ichoku et al. (2001). Averaged AOD values are used corresponding to an overpass time of ±30 min from the AERONET observation. AOD values derived from AVHRR data were averaged to an area of 50 km × 50 km around the AERONET sites, with the exclusion of pixels where the AVHRR-derived AOD had a standard deviation larger than 0.18 in the 50 km × 50 km window. The reason for exclusion of these pixels with a high AOD standard deviation is to avoid cloud-contaminated pixels. On the other hand, we reduce the number of LUT in term of the polynomial by the consideration of single scattering approximation to correct for the different solar and viewing geometries and this approximation is valid for low AOD, but deviates for larger AOD. The deviations start at AOD larger than 1.0 and increase with increasing wavelength.

There are only three AERONET sites located in/near Beijing, so there is only limited dataset for the validation. For the comparison, shown in Fig. 8, twenty-seven match-ups

AMTD
6, 2227–2251, 2013

Title Page
Abstract Introduction
Conclusions References
Tables Figures
◀ ▶
Back Close
Full Screen / Esc
Printer-friendly Version
Interactive Discussion

were found for the months of June and July in the years 2006–2011. The correlation coefficient is 0.861, but there is a high bias (around 0.15) and a slope of 0.764. The underestimation is due to the occurrence of absorbing aerosol in the study area which is not included in the BAER LUTs used in the retrieval. Figure 8 also shows that over Xianghe the AOD is sometimes overestimated, which was caused by the underestimation of surface reflectance as shown in Fig. 4. Cloud contamination may also be a factor here. However, due to the limited number of reference points available for this study area, we cannot properly evaluate the retrieval algorithm over this region. For the limited number of match-ups available, AVHRR AODs agree quite well with AERONET AOD while the spatial standard derivation calculated from AVHRR data is similar with the temporary standard deviation obtained from AERONET observation.

The statistical coefficient derived from MODIS data for the relation between the surface reflectances at 0.64 and 2.1 µm is used as prior knowledge in our retrieval method. However, we need to find the empirical relationships for different surface types and in different seasons. Figure 9, as an example, shows the AOD distribution over China derived from AVHRR and MODIS data. We can see that the AOD distribution from AHVRR and MODIS agree quite well over central and east China. However, over the west of China, the AVHRR overestimates the AOD. This is mainly due to the surface properties: the surface over the west of China is very bright and the dark surface assumption does not apply. Equation (12) may also be invalid for this bright region. As a result, the surface reflectance is underestimated which in turn cause overestimation of the AOD.

4 Conclusion

An aerosol retrieval algorithm has been presented which uses the single visible band of AVHRR, with support from the infrared channel to determine the surface reflectance. The main problem in aerosol retrieval from AVHRR data is that only one visible wavelength is available. Besides, there are two main limitations for the algorithm presented

AMTD
6, 2227–2251, 2013

in the paper. The first one is the effect from the emissivity, which may affect the surface reflectance at 3.75 µm. This effect will not be a great issue for a small study area as used in the study presented here because for such a small area the surface properties are expected be relatively constant. However, for larger areas we need the support of an emissivity dataset. The other problem is that a simple LUT was used which has been derived based on a phase function measured during the Lace experiment in 1998 (Von Hoyningen-Huene et al., 2003, 2011) and this phase function may not be representative for the situation over the Beijing area, especially as regards aerosol absorption. The developed algorithm is the first promising steps towards the retrieval of AOD from AVHRR data over land.

Acknowledgements. This work was partly supported by the National Natural Science Foundation of China (NSFC) under Grant No. 41271371, the Major International Cooperation and Exchange Project of NSFC (Grant No. 41120114001), and the Ministry of Science and Technology (MOST) of China under Grant No. 2009CB723906. The authors also thanks for the help of dealing with MOD09 data from Fei Li from Institute of Remote Sensing Application, Chinese Academy of Sciences. Thanks for Chi Li from Center for Earth Observation and Digital Earth of the Chinese Academy of Sciences for pre-processing two months dataset. The author appreciates the valuable comments from Jie Guang from Institute of Remote Sensing Application, Chinese Academy of Sciences. L. L. Mei would like to thank the Director Prize from the Institute of Remote Sensing Applications of Chinese Academy of Sciences. AVHRR data were available through NOAA (http://www.nsof.class.noaa.gov/saa/products/welcome), MODIS data were available through NASA (http://modis.gsfc.nasa.gov/) and meteorological data came from (http://envf.ust.hk/dataview/gts/current/query_gts_series.py?src_type=ax). Many thanks are due to the PI investigators with the AERONET sites used in this paper. Alexander Kokhanovsky acknowledges the support of the DFG Projects Terra and RESINC-II.

References

Allen, R. C., Durkee, P. A., and Wash, C. H.: Snow/cloud discrimination with multispectral satellite measurements, J. Appl. Meteorol., 29, 994–1004, 1990.

Brindley, H. E. and Ignatov, A.: Retrieval of mineral aerosol optical depth and size information from eteosat Second Generation SEVIRI solar reflectance bands, Remote Sens. Environ., 102, 344–363, 2006.

Bulgin, C. E., Palmer, P. I., Merchant, C. J., Siddans, R., Gonzi, S., Poulsen, C. A., Thomas, G. E., Sayer, A. M., Carboni, E., Grainger, R. G., Highwood, E. J., and Ryder, C. L.: Quantifying the response of the ORAC aerosol optical depth retrieval for MSG SEVIRI to aerosol model assumptions, J. Geophys. Res., 116, D05208, doi:10.1029/2010JD014483, 2011.

Chandrasekhar, S.: Raditive Trasfer, London (Oxford University Press), 1950.

Curier, L., de Leeuw, G., Kolmonen, P., Sundstrom, A.-M., Sogacheva, L., and Bennouna, Y.: Aerosol retrieval over land using the (A)ATSR dual-view algorithm, in: Satellite Aerosol Remote Sensing Over Land, edited by: Kokhanovsky, A. A. and de Leeuw, G., Praxis Publishing, Chichester, UK, 135–160, 2009.

de Leeuw, G., Kinne, S., Leon, J. F., Pelon, J., Rosenfeld, D., Schaap, M., Veefkind, P. J., Veihelmann, B., Winker, D. M., and von Hoyningen-Huene, W.: Retrieval of aerosol properties, in: The Remote Sensing of Tropospheric Composition from Space, edited by: Burrows, J. P., Platt, U., and Borrell, P., Springer-Verlag, Berlin, Heidelberg, ISBN: 978-3-642-14790-6, doi:10.1007/978-3-642-14791-3, 359–313, 2011.

Diner, D. J., Martonchik, J. V., Kahn, R. A., Pinty, B., Gobron, N., Nelson, D. L., and Holben, B. N.: Using angular and spectral shape similarity constraints to improve MISR aerosol and surface retrievals over land, Remote Sens. Environ., 94, 155–171, 2005.

Flowerdew, R. J. and Haigh, J. D.: An approximation to improve accuracy in the derivation of surface reflectances from multi-look satellite radiometers, Geophys. Res. Lett., 22, 1693–1696, 1995.

Frohlich, C. and Shaw, G. E.: New determination of Rayleigh scattering in the terrestrial atmosphere, Appl. Optics, 19, 1773–1775, 1980.

Guinot, B., Cachier, H., Sciare, J., Yu, T., Wang, X., and Yu, J. H.: Beijing aerosol: atmospheric interactions and new trends, J. Geophys. Res., 112, D14314, doi:10.1029/2006JD008195, 2007.

AMTD

6, 2227–2251, 2013

Retrieval of aerosol optical depth over land surfaces from AVHRR data

L. Mei et al.

Grey, W. M. F., North, P. R. J., Los, S. O., and Mitchell, R. M.: Aerosol optical depth and land surface reflectance from multi-angle AATSR measurements: global validation and inter-sensor comparisons, IEEE T. Geosci. Remote, 44, 2184–2197, 2006.
Hauser, A., Oesch, D., Foppa, N., and Wunderle, S.: NOAA AVHRR derived aerosol optical depth over land, J. Geophys. Res., 110, D08204, doi:10.1029/2004JD005439, 2005.
Holben, B. N., Vermote, E., Kaufman, Y. J., Tanre, D., and Kalb, V.: Aerosol retrieval over Land fromn AVHRR data-application for atmospheric correction, IEEE T. Geosci. Remote, 30, 212–222, 1992.
Holben, B. N., Eck, T. F., Slutsker, I., Tanre, D., Buis, J. P., Setzer, A. Vermote, E., Reagan, J. A., Kaufman, Y. J., Nakajima, T., Lavenu, F., Jankowiak, I., and Smirnov, A.: AERONET – a federated instrument network and data archive for aerosol characterization, Remote Sens. Environ., 66, 1–16, 1998.
Holzer-Popp, T., Schroedter-Homscheidt, M., Breitkreuz, H., Martynenko, D., and Kluser, L.: Benefits and limitations of the synergistic aerosol retrieval SYNAER, in: Satellite Aerosol Remote Sensing Over Land, edited by: Kokhanovsky, A. A. and de Leeuw, G., Praxis Publishing, Chichester, UK, 227–264, 2009.
He, K., Yang, F. M., Ma, Y. L., Zhang, Q., Yao, X. H., Chan, C. K., Cadle, S., Chan, T., and Mulawa, P.: The characteristics of $PM_{2.5}$ in Beijing, China, Atmos. Environ., 35, 4959–4970, 2001.
Ichoku, C., Chu, D. A., Mattoo, S., Kaufman, Y. J., Remer, L. A., Tanre, D., Slutsker, I., and Holben, B. N.: Techniques of global validation of aerosol retrievals from MODIS, in: Proceedings of the IEEE Geoscience and Remote Sensing Symposium held in Sydney, Australia, 9–13 July 2001, Vol. 3, IEEE, Piscataway, NJ, 1203–1205, doi:10.1109/IGARSS.2001.976792, 2001.
Ignatov, A.: Sensitivity and information content of aerosol retrievals from Advanced Very High Resolution Radiometer: Radiometric factors, Appl. Optics, 41, 991–1011, 2002.
Kokhanovsky, A. A. and de Leeuw, G. (Eds.): Satellite Aerosol Remote Sensing Over Land, Springer-Praxis, Berlin, ISBN 978-3-540-69396-3, 388 pp., 2009.
Kokhanovsky A. A., Mayer, B., and Rozanov, V. V.: A parameterization of the diffuse transmittance and reflectance for aerosol remote sensing problems, Atmos. Res., 73, 37–43, 2005.
Kaufman, Y. J., Tanre, D., Remer, L. A., Vermote, E. F., Chu, A., and Holben, B. N.: Operational remote sensing of tropospheric aerosol over land from EOS moderate resolution imaging spectroradiometer, J. Geophys. Res., 102, 17051–17067, doi:10.1029/96JD03988, 1997.

Knapp, K. R., Vonder Haar, T. H., and Kaufman, Y. J.: Aerosol optical depth retrieval from GOES-8: uncertainty study and retrieval validation over South America, J. Geophys. Res., 107, 4055, doi:10.1029/2001JD000505, 2002.

Knapp, K. P., Frouin, R., Kondragunta, S., and Prados, A.: Toward aerosol optical depth retrieval over land from GOES visible radiances: determining surface reflectance, Int. J. Remote Sens., 26, 4097–4116, 2005.

Kolmonen, P., Sundström, A.-M., Sogacheva, L., Rodriguez, E., Virtanen, T. H., and de Leeuw, G.: Towards the assimilation of the satellite retrieved aerosol properties: the uncertainty characterization of AOD for the AATSR ADV/ASV retrieval algorithm, Atmos. Meas. Tech. Discuss., in preparation, 2013.

Maignan, F., Breòn, F.-M., and Lacaze, R.: Bidirectional reflectance of Earth targets: valuation of analytical models using a large set of spaceborne measurements with emphasis on the Hop Spot, Remote Sens. Environ., 90, 210–220, 2004.

Mei, L. L., Xue, Y., de Leeuw, G., Holzer-Popp, T., Guang, J., Li, Y., Yang, L., Xu, H., Xu, X., Li, C., Wang, Y., Wu, C., Hou, T., He, X., Liu, J., Dong, J., and Chen, Z.: Retrieval of aerosol optical depth over land based on a time series technique using MSG/SEVIRI data, Atmos. Chem. Phys., 12, 9167–9185, doi:10.5194/acp-12-9167-2012, 2012.

Mei, L. L., Xue, Y., de Leeuw, G., von Hoyningen-Huene, W., Kokhanovsky, A. A., Istomina, L., Guang, J., and Burrows, J. P.: Aerosol optical depth retrieval in the Arctic region using MODIS data over snow, Remote Sens. Environ., 128, 234–245. doi:10.1016/j.rse.2012.10.009, 2013a.

Mei, L. L., Xue, Y., Kokhanovsky, A. A., von Hoyningen-Huene, W., Istomina, L., de Leeuw, G., Burrows, J. P., and Guang, J.: Aerosol optical depth retrieval over snow using AATSR data, Int. J. Remote Sens., in press, 2013b.

Riffler, M., Popp, C., Hauser, A., Fontana, F., and Wunderle, S.: Validation of a modified AVHRR aerosol optical depth retrieval algorithm over Central Europe, Atmos. Meas. Tech., 3, 1255–1270, doi:10.5194/amt-3-1255-2010, 2010.

Roger, J. C. and Vermote, E. F.: A method to retrieval the reflectivity signature at 3.75 µm from AVHRR data, Remote Sens. Environ., 64, 103–114, 1998.

Sundström, A.-M., Kolmonen, P., Sogacheva, L., and de Leeuw, G.: Aerosol retrievals over China with the AATSR dual-view algorithm, Remote Sens. Environ., 116, 189–198, 2012.

Tang, J. K., Xue, Y., Yu, T., and Guan, Y. N.: Aerosol optical thickness determination by exploiting the synergy of TERRA and AQUA MODIS, Remote Sens. Environ., 94, 327–334, 2005.

Takemata, K., Fukui, H., and Kawata, Y.: Retrieval of aerosol optical thickness over land using NOAA/AVHRR data, Adv. Space Res., 38, 2208–2211, 2006.

Von Hoyningen-Huene, W., Freitag, M., and Burrows, J. P.: Retrieval of aerosol optical thickness over land surface from top-of-atmosphere radiance, J. Geophys. Res., 108, 4260, doi:10.1029/2001JD002018, 2003.

Von Hoyningen-Huene, W., Kokhanovsky, A. A., Rozanov, V., Burrows, J. P., Hesselmans, G., Gale, L. and de Leeuw, G.: MSI aerosol retrieval algorithm for the Multi-Spectral mager (MSI) on EarthCare, in: ESA – Atmospheric Science Conference, Barcellona, 7–11 September 2009, available at: http://earth.eo.esa.int/workshops/atmos2009/participants/1283/pres_1283_vonHoyningenHuene_ppt.pdf (last access: 27 November 2012), 2009.

von Hoyningen-Huene, W., Yoon, J., Vountas, M., Istomina, L. G., Rohen, G., Dinter, T., Kokhanovsky, A. A., and Burrows, J. P.: Retrieval of spectral aerosol optical thickness over land using ocean color sensors MERIS and SeaWiFS, Atmos. Meas. Tech., 4, 151–171, doi:10.5194/amt-4-151-2011, 2011.

Xue, Y. and Cracknell, A. P.: Operational bi-angle approach to retrieve the Earth surface albedo from AVHRR data in the visible band, Int. J. Remote Sens., 16, 417–429, 1995.

Xue, Y., Guo, J. P., and Zhang, X. Y.: Aerosol optical thickness retrieval over non-Lambertian land surface with synergistic use of AATSR radiance measurements and MODIS derived albedo model parameters, Atmos. Res., 93, 736–746, 2009.

AMTD
6, 2227–2251, 2013

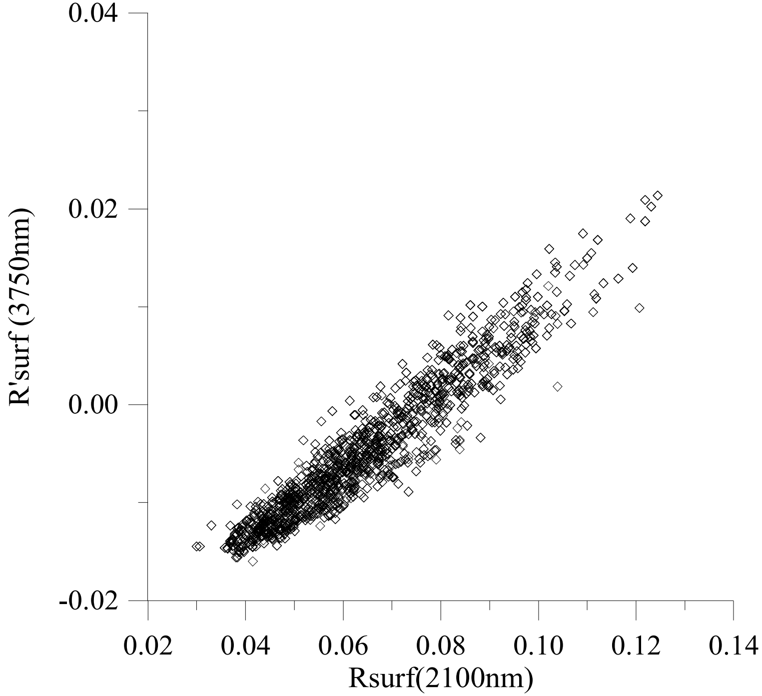

Fig. 1. Scatterplots of the TOA reflectances for the channels (a) R'_{Surf} (3.75 µm) (y-axis) with R_{Surf} (2.12 µm) (x-axis) from MODIS/AQUA for the Beijing region on 25 June 2008. Here we assume that the aerosol effect for 2.12 µm and 3.75 µm can be neglected, so the TOA reflectance is equal to the surface reflectance.

AMTD
6, 2227–2251, 2013

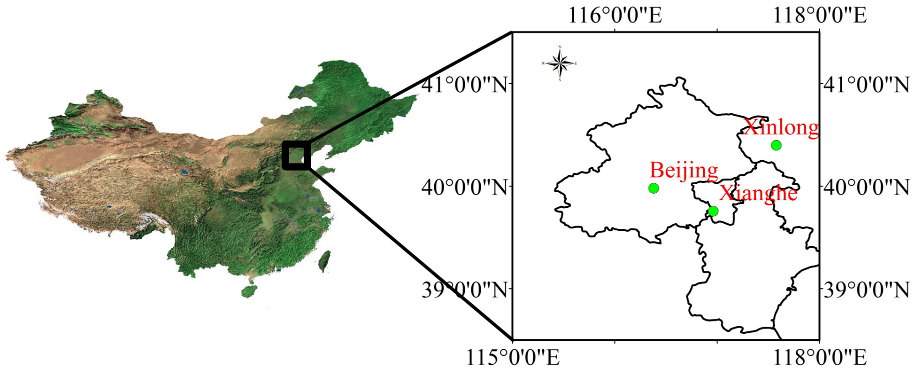

Fig. 2. Study area in the NE of China. The location of AERONET sites in this area is indicated.

AMTD
6, 2227–2251, 2013

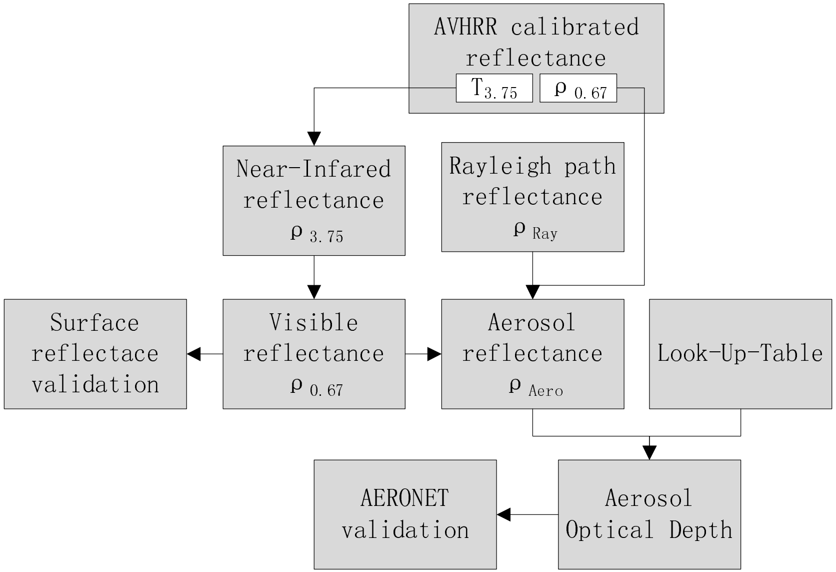

Fig. 3. Scheme of the main steps of AVHRR retrieval procedure.

AMTD
6, 2227–2251, 2013

Retrieval of aerosol optical depth over land surfaces from AVHRR data

L. Mei et al.

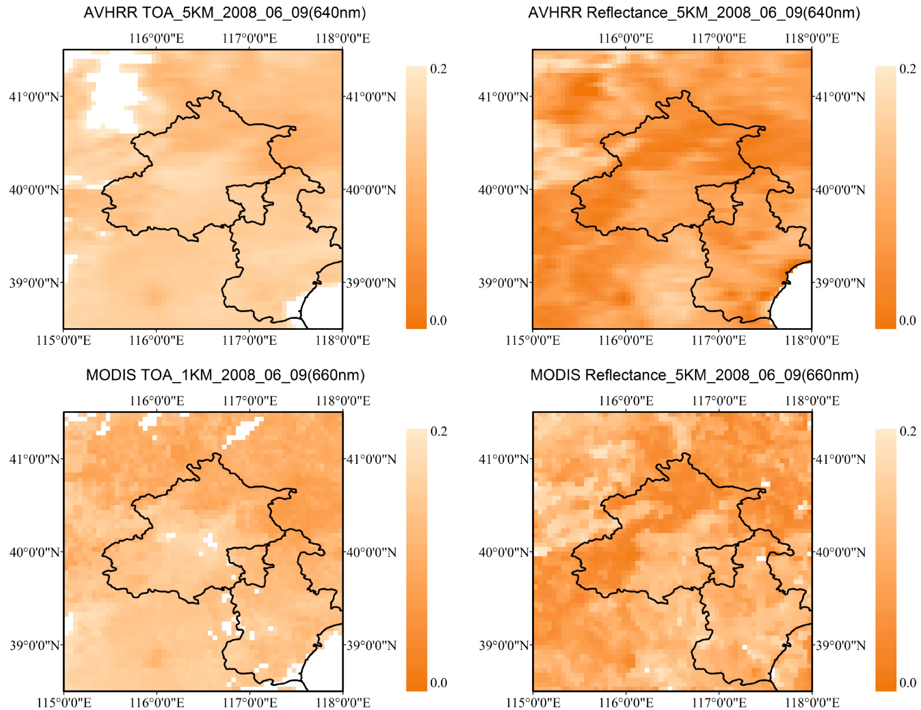

Fig. 4. TOA reflectances for AVHRR and MODIS on 9 June 2008 (the most bright surface is lack of data) are shown on the right, surface reflectances are shown at the right. Top row shows AVHRR data for a wavelength of 0.64 µm, bottom row shows MODIS data for a wavelength of 0.66 µm. The MODIS TOA data are presented with a resolution of 1km, while the surface reflectances are presented with a resolution of 5km to match the AVHRR data on the top row.

AMTD
6, 2227–2251, 2013

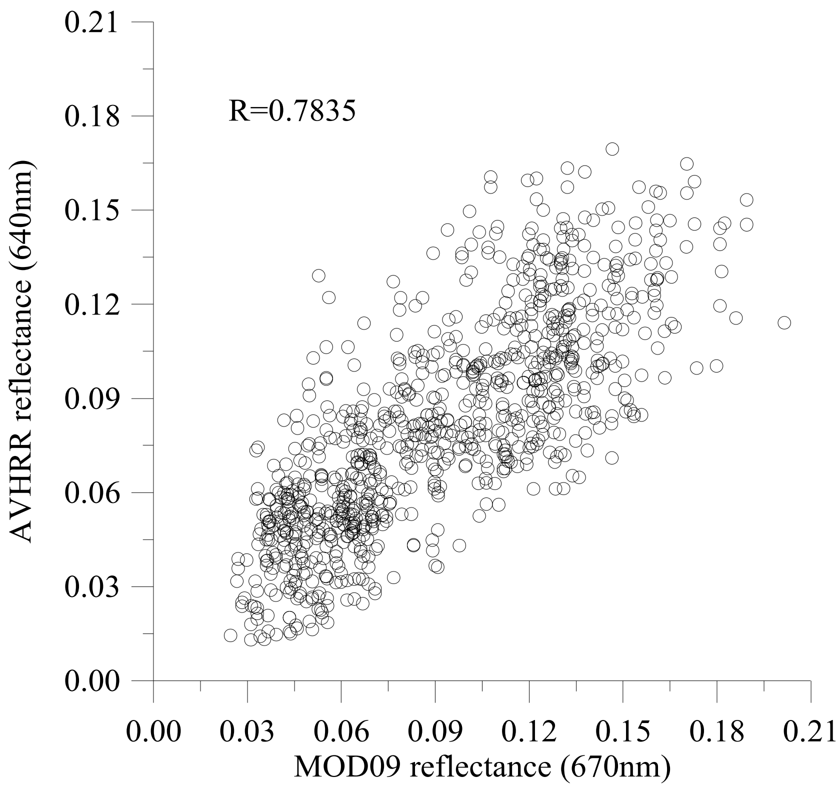

Fig. 5. Scatterplot between MODIS surface reflectance at 0.67 µm and AVHRR surface reflectance at 0.64 µm.

AMTD
6, 2227–2251, 2013

Retrieval of aerosol optical depth over land surfaces from AVHRR data

L. Mei et al.

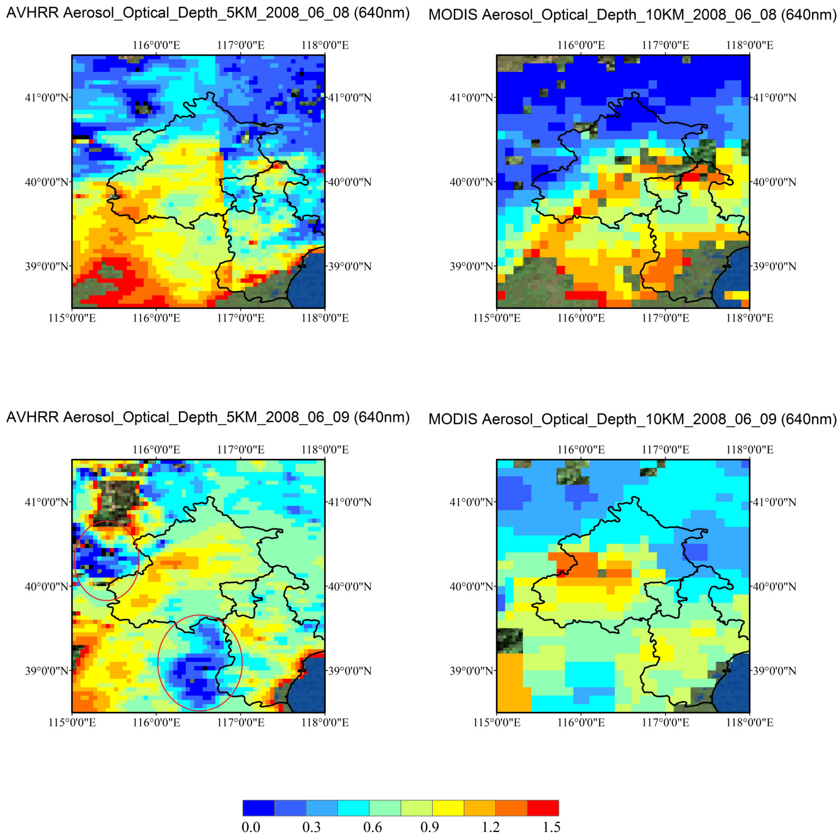

Fig. 6. Comparison between AVHRR derived-AOD (left column) and MODIS AOD product (Collection 5) (right column), for 8 (top) and 9 (bottom) June of 2008. The MODIS AOD at 0.64 µm was converted from AOD at 0.55 µm using fixed Angstrom coefficient ($\alpha = 1$). The line of AVHRR AOD figure on 8 June 2008 comes from the AVHRR TOA reflectance.

AMTD
6, 2227–2251, 2013

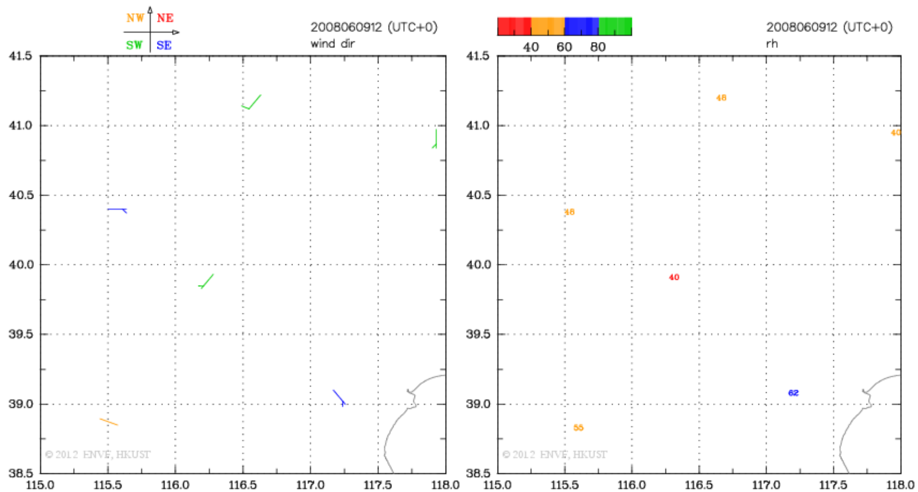

Fig. 7. Wind directions (left) and humidity (right) of study area on 9 June 2008 at 12:00 local time.

AMTD
6, 2227–2251, 2013

Retrieval of aerosol optical depth over land surfaces from AVHRR data

L. Mei et al.

Title Page
Abstract | Introduction
Conclusions | References
Tables | Figures
◀| |▶
◀ ▶
Back | Close
Full Screen / Esc
Printer-friendly Version
Interactive Discussion

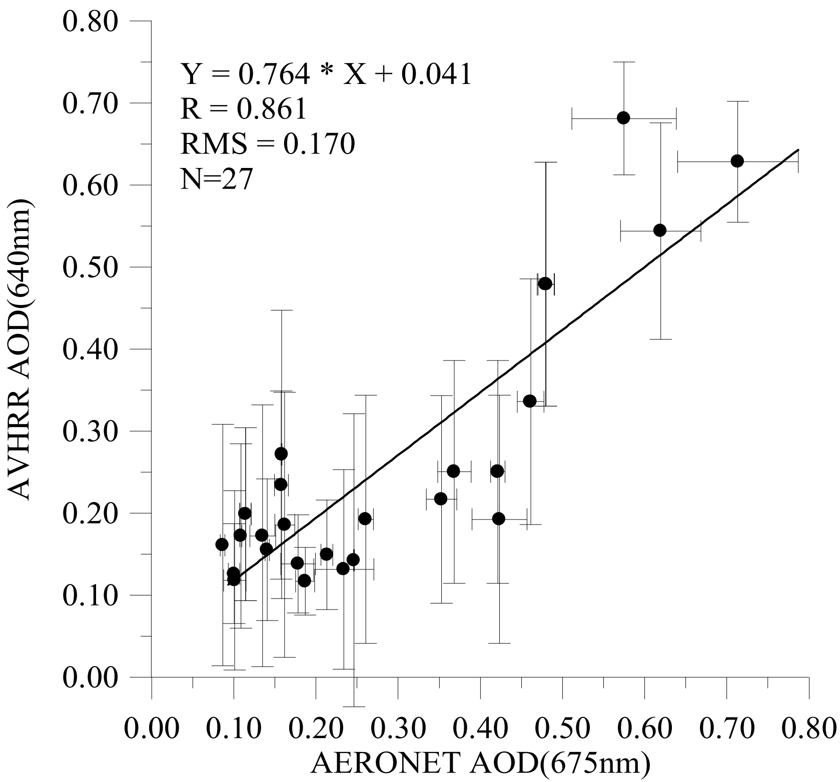

Fig. 8. Scatter plot of AVHRR-derived AOD (0.64 µm) versus AERONET AOD for 0.675 µm. Text at the top describes: the number of collocation (N), the regression curve, correlation (R), and the RMS error of the fit.

AMTD
6, 2227–2251, 2013

Title Page
Abstract | Introduction
Conclusions | References
Tables | Figures
◀I | ▶I
◀ | ▶
Back | Close
Full Screen / Esc
Printer-friendly Version
Interactive Discussion

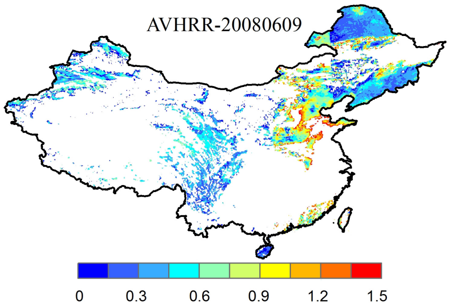

Fig. 9. Aerosol optical depth distribution of 0.64 µm from AVHRR and MODIS/TERRA over China on 9 June 2008. Here MODIS AOD at 0.64 µm was converted from AOD at 0.55 µm using fixed Angstrom coefficient ($\alpha = 1$).

AMTD
6, 2227–2251, 2013

Retrieval of aerosol optical depth over land surfaces from AVHRR data

L. Mei et al.